AJNR

Phase-Contrast MR Imaging Support for the Diagnosis of Aqueductal Stenosis

S. Stoquart-El Sankari, P. Lehmann, C. Gondry-Jouet, A. Fichten, O. Godefroy, M.-E. Meyer and O. Baledent

Phase-Contrast MR Imaging Support for the Diagnosis of Aqueductal Stenosis

S. Stoquart-El Sankari
P. Lehmann
C. Gondry-Jouet
A. Fichten
O. Godefroy
M.-E. Meyer
O. Baledent

BACKGROUND AND PURPOSE: Patients with aqueductal stenosis (AS) present with various clinical and radiologic features. Conventional MR imaging provides useful information in AS but depends on a subjective evaluation by the neuroradiologist. The purpose of this study was to evaluate the support of the phase-contrast MR imaging (PC-MR imaging) technique (sensitive to CSF flows) for the diagnosis of AS.

MATERIALS AND METHODS: We retrospectively considered 17 patients who underwent PC-MR imaging to explore hydrocephalus, with the absence of CSF flow at the aqueductal level. We analyzed their clinical and morphologic MR imaging data.

RESULTS: None of the usually reported direct or indirect signs of aqueductal obstruction were seen in 7 patients in whom the clinical suggestion of AS was confirmed by PC-MR imaging results. Seven patients in this population had a third ventriculostomy, and 5 of them were among those in whom conventional MR imaging failed to reveal signs of aqueductal obstruction. All of these 7 patients had a positive postsurgical outcomes. The analysis of CSF and vascular dynamic data in this population was compared with an aged-matched population, and these data were found similar except for the fourth ventricular CSF flush flow latency.

CONCLUSIONS: PC-MR imaging supports the diagnosis of CSF flow blockage at the aqueductal level in a reliable, reproducible, and rapid way, which aids in the diagnosis of AS in patients with clinical and/or radiologic suggestion of obstructive hydrocephalus. We, therefore, suggest using this technique in the current evaluation of hydrocephalus.

Noncommunicating hydrocephalus in adults remains a difficult diagnosis because of heterogeneous features. Aqueductal stenosis (AS) includes a large variety of etiologies: posthemorrhagic or postmeningitic obstruction, compression of the aqueduct, or presence of a third ventricle mass.[1] Patients with late-onset AS present with various clinical and radiologic features.[1-3] New theories have emerged about the pathogenesis of AS in adults, and venous hypertension has been suggested as the primary phenomenon responsible for ventricle dilation and aqueductal obstruction.[4] As a consequence, the determination of the underlying mechanism in hydrocephalus is relevant due to surgical implications because endoscopic third ventriculostomy (ETV) is mainly successful in obstructive hydrocephalus.[5,6]

Conventional MR imaging provides useful information in AS, because it may show triventricular dilation, CSF pathway obstruction at the aqueductal level on sagittal T2 sequences, downward bulging of the floor of the third ventricle (3rd V), anterior bulging of the 3rd V, etc.[7] Nevertheless, these criteria depend on a subjective evaluation by the neuroradiologist, may be difficult to assess in some patients, and thus are hardly comparable in postsurgical outcome studies.[6,8]

Phase-contrast MR imaging (PC-MR imaging) is a rapid, simple, and noninvading technique, which is sensitive to CSF flows.[9,10] In the past decade, the use of this technique has increased in the evaluation of cranial and spinal CSF flows, with considerable support in understanding the mechanical coupling between the cerebral blood and the CSF flows throughout the cardiac cycle (CC) and the temporal coordinated succession of these flows in healthy young subjects.[11-13] Greitz et al[14] considered that the intracranial blood and CSF flush and fill flows through the CC are initiated by the systolic intracerebral arterial inflow. Further studies, by using PC-MR imaging, proposed a dynamic model for mechanical coupling between blood and CSF intracranial flows.[11] The systolic arterial fill flow peak in the carotid arteries results in an instantaneous increase of the intracranial pressure. The first and faster way to decrease intracranial pressure is a large CSF venting in the subarachnoid spaces, which drops the cerebral subarachnoid space pressure. Then flush flows occur in the cerebral venous and aqueductal CSF compartments.

An imbalance in this mechanical coupling is presumed to be responsible for pathologic cerebral states,[15] such as normal pressure hydrocephalus (NPH)[16] or Alzheimer disease.[17] Despite technical controversies, CSF flow measurements at the aqueductal level have yielded considerable support for diagnosis and therapeutic decisions in communicating hydrocephalus.[18-20] Nevertheless, to our knowledge, this technique has never been evaluated in AS.

PC-MR imaging is usually added to conventional MR imaging examinations in our clinic when hydrodynamic intracerebral dysfunction is suggested, especially with triventricular dilation observed on morphologic MR imaging sequences. The purpose of this study was to evaluate the support of PC-MR imaging in the diagnosis of AS.

Materials and Methods

Subjects

Patients. We retrospectively considered all patients who underwent cranial PC-MR imaging for the evaluation of hydrocephalus in
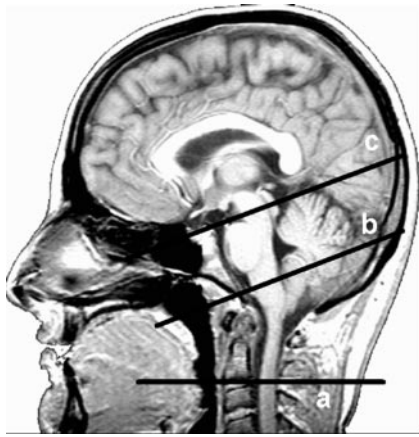
Fig 1. Sagittal scout view sequences are used as localizers to select the anatomic levels for flow quantification. The acquisition planes are selected perpendicular to the presumed direction of the flow. Sections through the C2–C3 subarachnoid space level (a), fourth ventricle (b), and Sylvian aqueduct (c) are used for CSF. By varying the velocity encoding, the same cervical section level (a) is used to measure vascular flows in the left and right internal carotid arteries, vertebral arteries, and internal jugular veins.

our unit since December 2006. Among this population, we selected patients in whom CSF sequences at the aqueductal level showed no aqueductal flow, and we reviewed their medical files and morphologic cerebral MR images. A medical history of meningitis or cranial malformation was extracted retrospectively from the medical records, as well as preoperative symptoms (headaches, gait disorders, intellectual deficiencies, seizures, etc). The duration between the onset of symptoms and radiologic evaluation was classified into 3 categories: 1) acute onset (within 1 month), 2) subacute onset (1–6 months), and 3) chronic onset (>6 months).

Controls. The control population consisted of 20 healthy volunteer adults who underwent an equivalent MR imaging protocol, with no clinical symptoms and no abnormalities detected on morphologic MR imaging sequences. Patients and controls were age-matched.

MR Imaging Data Acquisition

All patients had their hydrocephalus evaluated with a morphologic MR imaging of the brain. All MR imaging examinations were performed by using a 1.5T scanner (Signa; GE Healthcare, Milwaukee, Wis), with a phased-array head coil. Patients were supine. Conventional morphologic sequences were acquired in each patient, depending on the clinical request. At least both sagittal and axial T2 sequences were necessary and reread by a neuroradiologist blinded to the final diagnosis and to PC-MR imaging results.

All patients had PC-MR imaging sequences for blood and CSF flows added to the conventional clinical brain MR imaging protocol. Flow images were acquired with a 2D cine PC-MR imaging pulse sequence with retrospective peripheral gating so that the 16 frames analyzed covered the entire CC. Sagittal scout view sequences were used as localizers to select the anatomic levels for flow quantification. The acquisition planes were selected perpendicular to the presumed direction of the flow and are represented in Fig 1. Sections through the C2–C3 subarachnoid space level, the Sylvian aqueduct, and the fourth ventricle (4th V) levels were used for CSF, and sections through the C2–C3 level were used to measure vascular flows in left and right internal carotid arteries, vertebral arteries, and internal jugular veins. The acquisition time for each flow series was approximately 2 minutes, with slight fluctuation that depended on the participant's heart rate.

The MR imaging parameters were as follows: TE, 6–9 ms; TR, 20 ms; flip angle, 25° for vascular flows, 20° for CSF flows; FOV, 16 × 12 mm^2; matrix, 256 × 128; section thickness, 6 mm. Velocity (encoding) sensitization was set at 80 cm/s for the vascular flows, 10 cm/s for the aqueductal CSF flows, and 5 cm/s for the CSF at the cervical subarachnoid spaces and 4th V levels.

Data Analysis

Conventional MR Imaging Data. For each patient, the radiologist had to assess the following criteria:

1) Triventricular dilation defined by a dilation of both lateral ventricles and the 3rd V.

2) A comparatively small 4th V.

3) Direct visibility of CSF pathway obstruction at the aqueduct on sagittal T2 sequences (corresponding to the flow void sign).

4) Downward bulging of the floor of the 3rd V, defined by a displacement of the floor of the 3rd V of ≥5 mm from the line from the chiasma to the mamillary bodies.

5) A space-occupying lesion, in the 3rd V, in the pineal region or a posterior fossa tumor.

The radiologist had to score each item with 0 (absent), 1 (present), or 2 (unknown).

PC-MR Imaging Data. Data were analyzed by using an in-house image-processing software,[11] with an optimized CSF and blood-flow segmentation algorithm, which automatically extracts the region of interest at each level and calculates its flow curves over the 16 segments of the CC (for more details, refer to the description of the processing protocol in previous studies[11,21]).

Then, the mean venous, arterial, and CSF flow curves were generated. For the arterial flows, we calculated the mean cerebral arterial total blood flow in milliliters per minute, which was the sum of mean arterial flows in the left and right internal carotid and vertebral arteries. For the venous flows, a correction factor was applied to the amplitude of the internal jugular flow to obtain equality between the mean total inflow arterial and the mean total outflow venous rates, as described by previous works.[11,22]

The total cerebral vascular flow curve was generated by calculating the difference between arterial and venous flows throughout the CC. The time integral of this arteriovenous (AV) curve gave the intracranial blood volume change during the CC. The absolute sum of this volume maximum change in the caudal and cranial directions during the CC defined the "blood stroke volume" responsible for the dynamic coupling and succession of cerebral flows, starting with the CSF cervical venting. For the AV flow curve, we analyzed the AV delay (AVD), representing the latency between the arterial systolic inflow peak and the outflow venous peak. This AVD was represented in terms of percentage of CC, with the zero reference corresponding to the arterial inflow peak.

Similarly, CSF flow curves in the cervical and 4th V levels were integrated, providing the CSF stroke volumes, which represent the CSF volumes displaced in both directions through the considered region of interest at the corresponding level.[9,10] These volumes represent the "mobile compliance" of the subarachnoid and ventricular compartments and contribute to rapid regulation of intracranial pressure throughout the CC. By definition, all patients had no detected CSF flow at the aqueductal level. For each of these curves, amplitude and temporal characteristic parameters were analyzed. For CSF flow curves, the main parameters were those corresponding to the flush phase, and they were analyzed for both patients and control

Table 1: Clinical presentation in patients with AS

Symptoms	Acute Onset*	Subacute Onset†	Chronic Onset‡
Headache	5	4	1
Gait disturbance	0	1	6
Memory disturbance	0	1	6
Incontinence	0	1	5
Seizure	0	2	0

Note:—AS indicates aqueductal stenosis.
* Duration between symptoms and radiologic examination <1 month.
† Duration between 1 and 6 months.
‡ Chronic onset: duration >6 months. Numbers refer to patients in each category.

Table 2: Morphologic MR imaging results*

	Present	Absent	Unknown
Triventricular dilation	17	0	0
Small/normal 4th V	17	0	0
Direct CSF pathway obstruction (sagittal T2)	10	4	3
Downward bulging of the floor of the 3rd V	10	7	0
Space-occupying lesion	3	14	0

Note:— 4th V indicates fourth ventricle; 3rd V, third ventricle.
* Numbers refer to the patients in each category.

populations. All temporal parameters were expressed in terms of percentage of the CC.

Statistical Analysis

Amplitude and temporal parameters in patients were compared with those of the healthy age-matched control population by using a univariate analysis with a nonparametric Mann-Whitney *U* test. The level for statistical significance (*P* value) was set at .05.

Results

Clinical Results

Seventeen (mean age, 39 ± 4 years) patients fulfilled PC-MR imaging criteria for AS. They were matched with 20 healthy adult volunteers (mean age, 44 ± 24 years), who underwent an equivalent MR imaging protocol, with normal results.

Neurologic symptoms and disease duration in patients are summarized in Table 1. Medical history revealed 2 cases of meningitis in the childhood, 1 case of Arnold-Chiari type I malformation, and 1 case of spina bifida with surgery in childhood. Space-occupying lesions were found in 3 other patients. In these 7 patients, hydrocephalus was considered to be secondary.

Ten patients presented with unusual headaches, predominantly with an acute or subacute duration, and 7 patients, with gait and/or memory disturbance, principally with a chronic presentation. Three patients presented with the association of long-duration NPH symptoms and acute headaches related to acute intracranial hypertension.

Conventional MR Imaging Results

Conventional morphologic MR imaging sequences were retrospectively reviewed by a neuroradiologist blinded to the final diagnosis. Results are reported in Table 2.

Triventricular dilation with a comparatively small 4th V was found in all 17 patients, and space-occupying lesions were identified in 3 patients (2 peduncular astrocytomas, 1 pineal cyst). None of the other direct or indirect signs of aqueductal obstruction were seen in 7 patients, in whom the clinical sug-
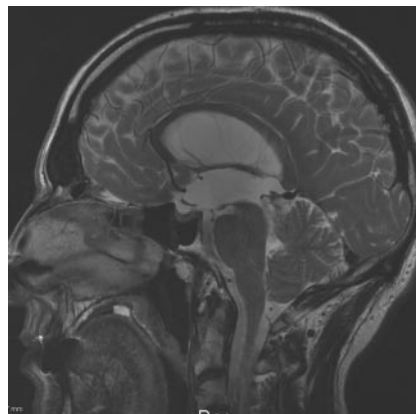

Fig 2. Sagittal T2 conventional MR image in a 50-year-old patient admitted for recent gait and urinary dysfunction, with a medical history of chronic headaches. Note the dilated lateral and 3rd Vs associated with a comparatively small 4th V. There is a slight downward bulging of the floor of the 3rd V, but no direct signs of obstruction at the aqueductal level. PC-MR imaging (not shown) showed a total absence of CSF flow at the aqueductal level and helped the neurosurgeon with the diagnosis of aqueductal stenosis.

Table 3: Amplitude and temporal parameters of vascular blood flow and CSF (cervical and ventricular) flows in patients with AS and controls*

	AS	Control	P
No. of patients	17	20	NS
Age (yr)	39	44	NS
Vascular flows			
Arterial mean flow (mL/min)	589 ± 115	607 ± 158	NS
Venous mean flow (mL/min)	379 ± 157	417 ± 158	NS
Arteriovenous delay (% of CC)	16 ± 12	19 ± 12	NS
Arteriovenous stroke volume (mL)	0.8 ± 0.2	0.8 ± 0.3	NS
Cervical flows			
C2–C3 peak flush flow (mL/min)	157 ± 58	160 ± 54	NS
C2–C3 peak flush latency (% of CC)	6 ± 3	5 ± 4	NS
C2–C3 stroke volume (μL/CC)	499 ± 251	508 ± 166	NS
4th V flows			
4th V peak flush latency (% CC)	4 ± 7	13 ± 8	.05
4th V stroke volume (μL/CC)	24 ± 18	24 ± 13	NS
Aqueductal level			
Stroke volume (μL/CC)	∅	44 ± 25	

Note:—NS indicates no significance; ∅, absence of flow.
* Results are represented by mean ± SD values.

gestion of AS was confirmed by PC-MR imaging results (Fig 2).

Seven patients in this population had an ETV, and 5 of them were among those in whom conventional MR imaging failed to reveal either direct or indirect signs of aqueductal obstruction. All of these 7 patients had a positive postsurgical outcome, with complete recovery of clinical symptoms and a follow-up duration longer than 1 year in all of them.

PC-MR Imaging Results

The mean flow curves of patients with AS and healthy controls were generated for aqueductal, 4th V, and cervical CSF, as well as for arterial, venous, and AV flows. The mean values of key parameters of arterial, venous, and AV blood flows in patients and control groups are shown in Table 3. Temporal and amplitude vascular data were comparable in the 2 populations, except for the AVD, which was significantly (*P* < .01) reduced in patients with AS in comparison with controls (respectively, 7.7 ± 3.2% and 14.9 ± 5.9% of CC). Considering the cervical

flow parameters, there were no statistical differences between the patients with AS and the adult controls.

For ventricular CSF flows, as expected, aqueductal stroke volume was null in all patients with AS and normal in the control population. Most interesting, at the 4th V level, stroke volumes were similar in both populations, but the CSF flush peak occurred significantly ($P < .05$) earlier in patients with AS ($4 \pm 7\%$) than in controls ($13 \pm 8\%$).

Discussion

AS diagnosis may be difficult in adults because of various clinical, etiologic, and radiologic features. Patients with late-onset AS may present with chronic hydrocephalus symptoms (gait, cognitive, or urinary disturbance), which can mimic the Hakim triad of NPH.[1,3] In other patients, obstruction of CSF pathways may remain well tolerated for years and may be revealed by an acute intracranial hypertensive syndrome.[3] This heterogeneity of clinical presentation is well represented in our AS population. Additionally, AS may be either idiopathic or related to secondary etiologies (arachnoiditis, cervical malformations, posterior fossa tumors).[1] Furthermore, aqueductal aspects in AS are various, as has been emphasized in an earlier ventriculography study: club-shaped end, broad funnel, narrow funnel, membranous aqueduct, or aqueduct atresia are some of described AS configurations.[23]

Additionally, new theories have emerged in the past decades, based on the Monro-Kellie doctrine, stating that the intracranial pressure equilibrium is related to a mechanical coupling between the vascular, brain tissue, and CSF intracranial compartments. The most studied pathologic model has been NPH, and hypotheses about CSF cervical resorption or venous drainage alterations have been suggested as the underlying mechanisms for communicating hydrocephalus.[14,24] More recently, some authors[4,24] have suggested similar mechanisms in obstructive hydrocephalus. These studies were based on animal models: The ventricular injection of kaolin clay resulted in inflammation of the meninges and, therefore, CSF resorption troubles.[25] For these authors, an increased pressure in the venous system (particularly in the sagittal sinus) resulted in brain compliance decrease and was responsible for aqueductal blockage and ventricle dilation.[4]

All of these features make it difficult to assess the obstruction of CSF pathways in AS, which is relevant in patients because ETV is mainly successful in obstructive hydrocephalus.[5,6] Furthermore, a recent study tried to define predictors of good outcomes of ETV and proposed an objective grading system, independent of clinical and etiologic data, based on morphologic MR imaging criteria.[7] However, we think that the first step should be to provide a reliable diagnosis of obstructive hydrocephalus to select the appropriate surgical treatment. In 1967, a study used radiologic features on ventriculography to define signs and different shapes of AS.[23] Nevertheless, radiologic investigation of hydrocephalus currently relies on MR imaging examinations, and heterogeneous studies use variable and nonvalidated criteria to define AS: triventricular dilation with a relatively small 4th V, periventricular signs of CSF active resorption, the presence of a space-occupying lesion, a downward bulging of the 3rd V, and the absence of the flow void sign.

First, the presence of dilated lateral and 3rd Vs, out of pro-

portion for cortical atrophy, associated with a comparatively small 4th V has been proposed as suggestive of AS. This criterion was present in all of our patients, but one can argue that it is not a reproducible parameter, especially because no cutoff value for a "comparatively small 4th V" is available, particularly in patients with mild hydrocephalus.[3]

Second, the absence of a flow void signal intensity on sagittal T2 MR images has been proposed as a direct sign of CSF pathway obstruction at the aqueductal level. Nevertheless, the flow void signal intensity depends on several parameters (aqueductal diameter, CSF velocity, section thickness) and may be weak or absent if the aqueduct is physiologically narrow.[8] In our study, this criterion failed in 7 patients of 17 (it was absent in 4 patients and difficult to determine in 3). A direct visualization of aqueductal obstruction was found in 3 patients only (tectal tumor, pineal cyst). This parameter is of great value because it proves the obstructive nature of hydrocephalus. However, idiopathic AS is frequent, and checking for indirect signs of obstruction is usually recommended.[7]

Downward bulging of the floor of the 3rd V, underneath the line from the chiasma to the mamillary bodies, has been proposed as a sign of a raised pressure gradient between the 3rd V and the prepontine cistern and, thus, as an indirect sign of AS.[7] In our population, this sign was absent in 7 patients with AS. Because it depends on both the pressure difference between the 2 compartments and on its duration, the downward bulging may be slight if the pressure gradient is low or of a short duration. Besides, the bulging may be difficult to measure in this region, because it may be hindered in posthemorrhagic or postmeningitic AS.[7]

All of these direct or indirect signs are operator-dependent, difficult to reproduce, and lack validated cutoff values. On the other hand, PC-MR imaging can be used for neurologic and neurosurgical features to assess intracerebral and cervical CSF flows in qualitative and quantitative evaluations.[9-11,18,20,26] PC-MR imaging enables reliable, noninvading, and rapid measurements of CSF flows and is sensitive even to slow CSF flows as seen at the aqueductal level.[10,27]

In our study, PC-MR imaging revealed alteration of CSF circulation, in particular aqueductal obstruction in the 17 patients, whereas 7 of these patients had no certain direct or indirect signs of obstructive hydrocephalus on conventional cerebral MR images. Furthermore, 7 patients in our population had undergone ETV, with good clinical outcome at 1 year (improvement of headaches or gait/memory disturbance). Five of these patients did not have any of the direct/indirect criteria for AS on their cerebral morphologic MR images, and the surgical decision was helped by PC-MR imaging results. In most reports, ETV success rates were important, up to 78%.[28,29] However, the follow-up periods were limited, and the specific evaluation of nonresponsiveness and related factors was not addressed.

In a recent study,[30] the authors aimed to investigate these factors and assessed patients after ETV, for at least 1-year follow-up duration, with neurologic, neuropsychological, and radiologic evaluations. They found an improvement rate of 50% only and suggested that discrepancies with previous studies were related to longer follow-up duration, strict chosen criteria for improvement, and younger patients at surgery. In our opinion, these issues still are unclear because the primary

mechanisms of obstructive hydrocephalus remain incompletely understood. Additionally, 2 groups of patients emerge after treatment. In the first group, clinical and radiologic improvement was observed in late follow-up (up to several years). In the second group, an associated alteration of CSF resorption (which may be due to venous drainage dysfunction or subarachnoid CSF drainage abnormalities) resulted in clinical worsening and the need for a ventriculoperitoneal shunt.[31]

On the other hand, limits of PC-MR imaging can be discussed. First, aqueductal CSF evaluation may be hampered by the small size of the aqueduct and ventricular foramina. However, previous phantom studies[27,32] supported good reliability and reproducibility of PC-MR imaging in evaluating CSF flows at the aqueductal level. Furthermore, in a previous study comparing our semiautomated CSF segmentation algorithm and manual tracing, CSF pulsatile patterns were homogeneous when processed in the narrow part of the aqueduct where velocity dispersion is minimized.[11]

Besides, one can argue that previous studies have shown a wide physiologic range of temporal, velocity, and flow CSF parameters in evaluated populations,[8] which are probably interoperator variations due to different acquisition and analysis protocols. Nevertheless, in all of our patients, the CSF flow was equal to zero at the aqueductal level.

Finally, in our experience, PC-MR imaging results for CSF flows can be hampered if a tap test was administered in the previous weeks because CSF removal decreases CSF oscillations. We, therefore, suggest that this technique should be performed before CSF removal.

As a conclusion, PC-MR imaging shows the absence of CSF flow at the aqueductal level in a reliable, reproducible, and rapid (1 minute) way, which supports the diagnosis of AS in patients with clinical and/or radiologic suggestion of obstructive hydrocephalus. We, therefore, recommend using this technique in the evaluation of hydrocephalus.

Additionally, PC-MR imaging provides vascular and CSF flow data and adds to the knowledge of the mechanical coupling between the cerebral blood and the CSF flows throughout the CC and their temporal coordinated succession, which is helpful for understanding the pathophysiology of hydrocephalus. In our study, patients had vascular, temporal, and volumetric flow data comparable with those of age-matched controls, as well as CSF flow values at the cervical and 4th V levels. The sole parameters modified in patients with AS were a decreased latency of occurrence of 4th V flush peak and a 50% reduction of AVD. These results are interesting because they suggest that there is an intracranial cerebral compliance adaptation to chronic obstruction of CSF pathways. Bateman[24] found similar results in patients with NPH, by measuring the AVD, which was significantly reduced, corresponding to the venous flush occurring earlier in the CC. In a recent study, this author showed similar results (with AVD reduced up to 50%) in patients with obstructive hydrocephalus, suggesting that the underlying mechanism may be the same in NPH and AS.[4] In this study, because the arterial inflow was preserved in patients with AS, the AVD reduction was supposed to be related to increased resistance in venous drainage pathways. It would also be interesting to compare flow results in patients before and after ETV.

Conclusions

AS diagnosis remains difficult because of heterogeneous clinical and etiologic features. Morphologic MR imaging examinations provide direct or indirect signs suggesting AS, but to our knowledge, these signs have never been validated and seem to be difficult to use, especially in postsurgical outcome evaluations. We suggest the complementary use of rapid, easy, and reproducible PC-MR imaging sequences, to prove the obstruction of CSF circulation at the aqueductal level.

References

1. Little JR, Houser OW, MacCarty CS. **Clinical manifestations of aqueductal stenosis in adults.** *J Neurosurg* 1975;43:546–52
2. Harrison MJ, Robert CM, Uttley D. **Benign aqueduct stenosis in adults.** *J Neurol Neurosurg Psychiatry* 1974;37:1322–28
3. Fukuhara T, Luciano MG. **Clinical features of late-onset idiopathic aqueductal stenosis.** *Surg Neurol* 2001;55:132–36, discussion 136–37
4. Bateman GA. **Magnetic resonance imaging quantification of compliance and collateral flow in late-onset idiopathic aqueductal stenosis: venous pathophysiology revisited.** *J Neurosurg* 2007;107:951–58
5. Foroutan M, Mafee MF, Dujovny M. **Third ventriculostomy, phase-contrast cine MRI and endoscopic techniques.** *Neurol Res* 1998;20:443–48
6. Kim SK, Wang KC, Cho BK. **Surgical outcome of pediatric hydrocephalus treated by endoscopic III ventriculostomy: prognostic factors and interpretation of postoperative neuroimaging.** *Childs Nerv Syst* 2000;16:161–68, discussion 169
7. Kehler U, Regelsberger J, Gliemroth J, et al. **Outcome prediction of third ventriculostomy: a proposed hydrocephalus grading system.** *Minim Invasive Neurosurg* 2006;49:238–43
8. Schroeder HW, Schweim C, Schweim KH, et al. **Analysis of aqueductal cerebrospinal fluid flow after endoscopic aqueductoplasty by using cine phase-contrast magnetic resonance imaging.** *J Neurosurg* 2000;93:237–41
9. Nitz WR, Bradley WG Jr, Watanabe AS, et al. **Flow dynamics of cerebrospinal fluid: assessment with phase-contrast velocity MR imaging performed with retrospective cardiac gating.** *Radiology* 1992;183:395–405
10. Enzmann DR, Pelc NJ. **Cerebrospinal fluid flow measured by phase-contrast cine MR.** *AJNR Am J Neuroradiol* 1993;14:1301–07, discussion 1309–10
11. Baledent O, Henry-Feugeas MC, Idy-Peretti I. **Cerebrospinal fluid dynamics and relation with blood flow: a magnetic resonance study with semiautomated cerebrospinal fluid segmentation.** *Invest Radiol* 2001;36:368–77
12. Greitz D. **Cerebrospinal fluid circulation and associated intracranial dynamics: a radiologic investigation using MR imaging and radionuclide cisternography.** *Acta Radiol Suppl* 1993;386:1–23
13. Henry-Feugeas MC, Idy-Peretti I, Baledent O, et al. **Origin of subarachnoid cerebrospinal fluid pulsations: a phase-contrast MR analysis.** *Magn Reson Imaging* 2000;18:387–95
14. Greitz D, Wirestam R, Franck A, et al. **Pulsatile brain movement and associated hydrodynamics studied by magnetic resonance phase imaging: The Monro-Kellie doctrine revisited.** *Neuroradiology* 1992;34:370–80
15. Greitz T. **Effect of brain distension on cerebral circulation.** *Lancet* 1969;1:863–65
16. Greitz D. **Radiological assessment of hydrocephalus: new theories and implications for therapy.** *Neurosurg Rev* 2004;27:145–65, discussion 166–147
17. Uftring SJ, Chu D, Alperin N, et al. **The mechanical state of intracranial tissues in elderly subjects studied by imaging CSF and brain pulsations.** *Magn Reson Imaging* 2000;18:991–96
18. Bradley WG Jr, Scalzo D, Queralt J, et al. **Normal-pressure hydrocephalus: evaluation with cerebrospinal fluid flow measurements at MR imaging.** *Radiology* 1996;198:523–29
19. Bradley WG Jr. **MR prediction of shunt response in NPH: CSF morphology versus physiology.** *AJNR Am J Neuroradiol* 1998;19:1285–86
20. Baledent O, Gondry-Jouet C, Stoquart-Elsankari S, et al. **Value of phase contrast magnetic resonance imaging for investigation of cerebral hydrodynamics.** *J Neuroradiol* 2006;33:292–303
21. Stoquart-El Sankari S, Baledent O, Gondry-Jouet C, et al. **Aging effects on cerebral blood and cerebrospinal fluid flows.** *J Cereb Blood Flow Metab* 2007;27:1563–72
22. Alperin N, Vikingstad EM, Gomez-Anson B, et al. **Hemodynamically independent analysis of cerebrospinal fluid and brain motion observed with dynamic phase contrast MRI.** *Magn Reson Med* 1996;35:741–54
23. Schechter MM, Zingesser LH. **The radiology of aqueductal stenosis.** *Radiology* 1967;88:905–16
24. Bateman GA. **Vascular compliance in normal pressure hydrocephalus.** *AJNR Am J Neuroradiol* 2000;21:1574–85
25. Edvinsson L, West KA. **The time-course of intracranial hypertension as re-**

corded in conscious rabbits after treatment with different amounts of intra-cisternally injected kaolin. *Acta Neurol Scand* 1971;47:439–50

26. Egeler-Peerdeman SM, Barkhof F, Walchenbach R, et al. **Cine phase-contrast MR imaging in normal pressure hydrocephalus patients: relation to surgical outcome.** *Acta Neurochir Suppl* 1998;71:340–42

27. Barkhof F, Kouwenhoven M, Scheltens P, et al. **Phase-contrast cine MR imaging of normal aqueductal CSF flow: effect of aging and relation to CSF void on modulus MR.** *Acta Radiol* 1994;35:123–30

28. Dalrymple SJ, Kelly PJ. **Computer-assisted stereotactic third ventriculostomy in the management of noncommunicating hydrocephalus.** *Stereotact Funct Neurosurg* 1992;59:105–10

29. Jones RF, Kwok BC, Stening WA, et al. **Third ventriculostomy for hydroceph-alus associated with spinal dysraphism: indications and contraindications.** *Eur J Pediatr Surg* 1996;6(suppl 1):5–6

30. Tisell M, Almstrom O, Stephensen H, et al. **How effective is endoscopic third ventriculostomy in treating adult hydrocephalus caused by primary aqueduc-tal stenosis?** *Neurosurgery* 2000;46:104–10, discussion 110–11

31. Bateman GA, Smith RL, Siddique SH. **Idiopathic hydrocephalus in children and idiopathic intracranial hypertension in adults: two manifestations of the same pathophysiological process?** *J Neurosurg* 2007;107:439–44

32. Luetmer PH, Huston J, Friedman JA, et al. **Measurement of cerebrospinal fluid flow at the cerebral aqueduct by use of phase-contrast magnetic resonance imaging: technique validation and utility in diagnosing idiopathic normal pressure hydrocephalus.** *Neurosurgery* 2002;50:534–43, discussion 543–34